Organic Luminescent Molecule with Energetically Equivalent Singlet and Triplet Excited States for Organic Light-Emitting Diodes

Keigo Sato,[1] Katsuyuki Shizu,[1] Kazuaki Yoshimura,[3] Atsushi Kawada,[4] Hiroshi Miyazaki,[1,4] and Chihaya Adachi[1,2]

[1]*Center for Organic Photonics and Electronics Research (OPERA), Kyushu University, 744 Motooka, Nishi, Fukuoka 819-0395, Japan*

[2]*International Institute for Carbon Neutral Energy Research (WPI-I2CNER), Kyushu University, 744 Motooka, Nishi, Fukuoka 819-0395, Japan*

[3]*Basic Research Laboratories, Nippon Steel Chemical Co., Ltd., 46-80 Nakabaru, Sakinohama, Tobata, Kitakyushu, Fukuoka 804-8503, Japan*

[4]*Functional Materials Laboratories, Nippon Steel Chemical Co., Ltd., 46-80 Nakabaru, Sakinohama, Tobata, Kitakyushu, Fukuoka 804-8503, Japan*

(Received 22 December 2012; published 10 June 2013)

We demonstrate an organic molecule with an energy gap between its singlet and triplet excited states of almost zero ($\Delta E_{ST} \sim 0$ eV). Such separation was realized through proper combination of an electron-donating indolocarbazole group and a diphenyltriazine electron-accepting moiety. Calculated and measured ΔE_{ST} were 0.003 and 0.02 eV, respectively. A total photoluminescence efficiency of 59% ± 2% with 45% ± 2% from a delayed component and 14% ± 2% from a prompt component was obtained for a doped film. Organic light emitting diodes containing this molecule as an emitting dopant exhibited an unexpectedly high external electroluminescence efficiency of $\eta_{EQE} = 14\% \pm 1\%$.

DOI: 10.1103/PhysRevLett.110.247401 PACS numbers: 78.60.Fi, 81.05.Fb

Organic luminescent materials are widely used in various consumer products such as highlighters, anticounterfeit banknotes, and detergents, as well as in biological and medical applications helping to make our daily life colorful, enjoyable, and safe [1]. In addition to their use as chemical products, recent development of organic materials from a new perspective has opened up a novel possibility for their use in optoelectronic devices [2,3]. In particular, the luminescence and unique semiconducting characteristics of organic materials can be combined, leading to the rapid development of organic semiconductor devices such as organic light emitting diodes (OLEDs) [3–5]. After extensive study of OLEDs for the past 20 years, electroluminescent (EL) materials have usually been classified by one of two mechanisms, fluorescence or phosphorescence, where radiative decay occurs from singlet or triplet excited states, respectively. OLEDs significantly accelerated the development of organic luminescence materials through attempts to maximize EL efficiency.

OLEDs possess attractive features such as high EL efficiency, high contrast, and low weight, so they are used in sophisticated flat panel displays and a wide variety of information terminals such as mobile phones and tablets. Recently, OLED applications have expanded to large TVs [6,7] and general lighting [8,9], demonstrating that they have become an essential technology for light-emitting electronics. One of the fascinating characteristics of OLEDs originates from the organic semiconducting materials within them that allow unlimited molecular design. We expect that improved understanding of molecular structures will reveal undeveloped functions that will further enhance OLED performance. Development of organic light-emitting semiconductor materials is important to maximize light emitting efficiency. The use of phosphorescent iridium (Ir) complexes overcame the limitation of exciton production efficiency through spin-orbit coupling, resulting in devices with very high external EL efficiency (η_{EQE}) of over 20% [10–12]. In fact, the high η_{EQE} of such phosphorescent complexes prompted commercialization of OLEDs.

Unfortunately, rare metals such as Ir and Pt are not the ideal choice for OLED emitters. They are unevenly distributed resources, expensive, and produce toxic waste [13]. In addition, the rather low solubility of these metal complexes in organic solvents and their long-term instability can be a problem for solution processing [14]. To produce OLED emitters without these drawbacks, we recently prepared novel light-emitting materials that realize high efficiency without using rare metal complexes by taking advantage of very efficient thermally activated delayed fluorescence (TADF) [15–22]. We designed emitters that promote triplet excitons into a singlet (S_1) excited state because they possess a very small energy gap (ΔE_{ST}) between S_1 and triplet (T_1) excited states, as shown in Fig. 1.

Although some molecules are already known to exhibit TADF, their efficiencies are generally quite low, so TADF has been assumed useless for practical applications. In the last few years, we have surveyed various candidates as TADF emitters and found the molecules that exhibit significant TADF, tin(IV) octaethylporphine difluoride (SnF_2OEP) [15], 2-biphenyl-4,6-bis(12-phenylindolo[2,3-a]carbazole-11-yl)-1,3,5-triazine (PIC-TRZ) [16], 2,4-bis{3-(9*H*-carbazol-9-yl)-9*H*-carbazol-9-yl}-6-phenyl-1,3,5-triazine (CC2TA) [17], spiro derivatives [19,20], phenoxazine derivatives [21], diphenylsulfone derivatives [22],

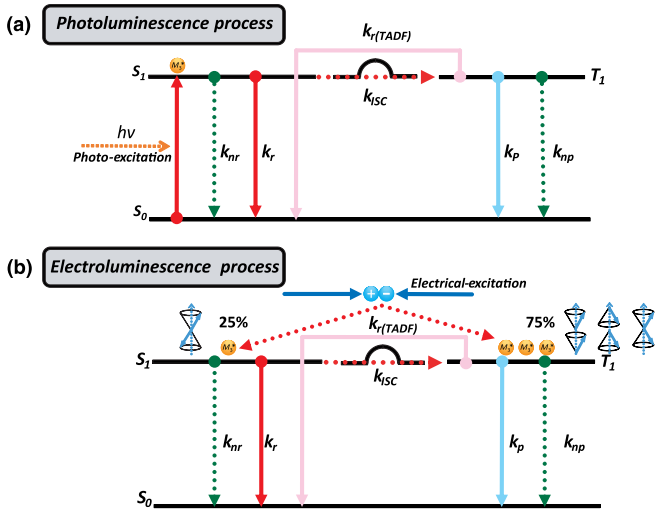

FIG. 1 (color online). Conceptual energy diagram of an organic luminescent molecule with a zero gap between the singlet (S_1) and triplet (T_1) excited states under (a) optical and (b) electrical excitations, including intersystem crossing forward and backward between the S_1 and T_1 excited states. In the photoluminescence process, singlet exciton formation occurs after photoexcitation. Some of the excitons decay radiatively and some convert to the T_1 state through intersystem crossing. Some of the triplet excitons then decay radiatively or nonradiatively to the ground state (S_0) and some upconvert to the S_1 state again through thermal upconversion. This process continues back and forth until the excitons reach a final thermal equilibrium. The upconverted singlet excitons decay through TADF. Under electrical excitation, excitons are directly formed as 75% triplet and 25% singlet, and the same exciton decay processes are followed. Thus, the large branching ratio of triplet excitons under electrical excitation is well harvested as light emission through TADF. (k_r is the fluorescence decay rate, k_r the nonradiative decay rate from the S_1 excited state, k_p the phosphorescence decay rate, k_{np} the nonradiative decay rate from the T_1 excited state, k_{ISC} the intersystem crossing rate, k_{RISC} the reverse intersystem crossing rate, M_1^* the singlet exciton, M_3^* the triplet exciton).

and dicyanobenzene derivatives [23]. While the first demonstration of TADF from SnF_2OEP with $\Delta E_{ST} = 0.24$ eV resulted in devices with a very low EL efficiency of 0.1%, it did show clear delayed EL resulting from the electrically generated TADF component. The second molecule, PIC-TRZ, possessed a rather small ΔE_{ST} of 0.1 eV and high η_{EQE} of 5.3%, which is significantly higher than the expected η_{EQE} of 2% considering only the photoluminescence (PL) efficiency of $\Phi_{PL} = 39\%$ related to conventional fluorescence [16]. Further, the improvement of ΔE_{ST} and η_{EQE} has been progressed, resulted in $\Delta E_{ST} = 0.06$ eV and $\eta_{EQE} = 11\%$ in CC2TA [17], $\Delta E_{ST} = 0.10$ eV and $\eta_{EQE} = 10\%$ in ACRFLCN [19], and $\Delta E_{ST} = 0.32$ eV and $\eta_{EQE} = 10\%$ in the diphenylsulfone derivative I [22]. In particular, the dicyanobenzene derivatives showed $\Delta E_{ST} = 0.083$ eV with a very high η_{EQE} of nearly 20%, indicating that the TADF concept is a promising technology in future OLEDs [23]. In this study, we further tried to expand TADF molecular structures focusing on the PIC-TRZ backbone that allows various modifications by designing the bonding manner of triazine and indrocarbazole units. During the survey of new molecular structures, we found an advanced molecule with an ultimately small ΔE_{ST} of ~0 eV, i.e., virtually zero gap. We believe that this is the first report on the molecules having zero-gap between the singlet and triplet excited states. An OLED containing this molecule exhibited a high η_{EQE} of 14% ± 1%.

In our successive design of TADF molecules, taking advantage of the backbone of PIC-TRZ, we systematically changed the number and position of an indolocarbazole unit while fixing the central triazine backbone and estimated ΔE_{ST} through density functional theory calculations. This allowed identification of the promising candidate 5,12-dihydro-12-(4,6-diphenyl-1,3,5-triazin-2-yl)-5-phenylindolo[3,2-a]carbazole (PIC-TRZ2) with $\Delta E_{ST} = 0.003$ eV, which is 1 order of magnitude smaller than that of PIC-TRZ ($\Delta E_{ST} = 0.080$ eV). Figure 2 shows the highest occupied molecular orbital (HOMO) and lowest unoccupied molecular orbital (LUMO) of PIC-TRZ and PIC-TRZ2. In the case of PIC-TRZ, the HOMO is localized over an indolocarbazole unit while the LUMO is located around a biphenyltriazine unit, indicating they are well separated. PIC-TRZ2 clearly showed better HOMO-LUMO separation than that of PIC-TRZ, so it is probable that the linear combination of one donor and one acceptor system in PIC-TRZ2 resulted in its small predicted ΔE_{ST}. It is the almost ideal separation of the HOMO and LUMO in PIC-TRZ2 that enables an ΔE_{ST} with almost zero gap.

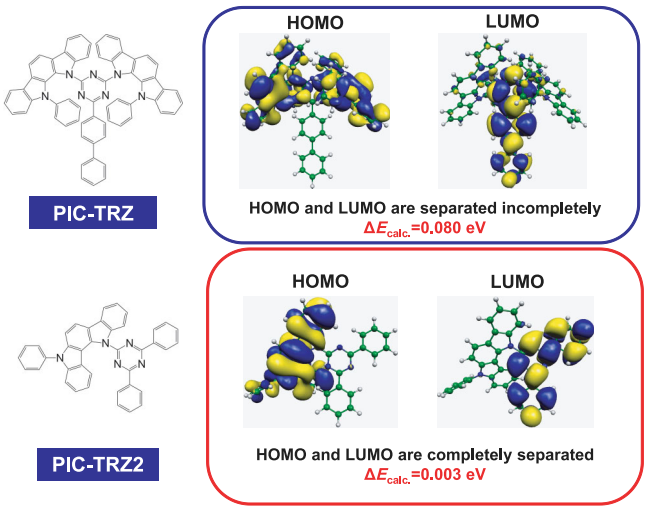

FIG. 2 (color online). Molecular structures of PIC-TRZ and PIC-TRZ2 with their HOMOs and LUMOs calculated at the PBE0/6-31G(d) level of theory. The calculated energy difference between the S_1 and T_1 excited states is $\Delta E_{calc} = 0.080$ eV for PIC-TRZ and 0.003 eV for PIC-TRZ2.

These promising characteristics calculated for PIC-TRZ2 prompted us to synthesize it, which we did following the procedure used to prepare PIC-TRZ.

Our goal is to achieve high TADF performance in a solid film, aimed for application in OLEDs, so we focused on host-guest systems containing a low concentration of guest to prevent concentration quenching. Figures 3(a) and 3(b) show transient PL decay and fluorescence [prompt component (black line)] and delayed fluorescence (red line) spectra of 6 wt %-PIC-TRZ2 doped into a 1,3-bis(carbazol-9-yl)benzene (mCP) host layer at $T = 5$ K. These spectra exhibit emission maxima at around 475 nm ($S_1 = 2.61$ eV), and overlap well with each other. Almost identical spectral behavior was observed at temperatures between 5 and 300 K. While the delayed component showed a nonexponential decay with a transient lifetime of a few ms at $T = 5$ K, as shown in Fig. 3(a), a single exponential decay gradually emerged as the temperature was increased. In the case of PIC-TRZ, although we clearly observed the appearance of phosphorescence at low temperature (below $T = 100$ K), demonstrating a characteristic emission spectrum with clear vibrational peaks [16], no such emission spectrum was observed for PIC-TRZ2. Thus, we conclude that the delayed component is related to TADF, and up-conversion occurs in PIC-TRZ2 even at $T = 5$ K, indicating it possesses virtually zero gap. The transient PL decay characteristics of PIC-TRZ2 at room temperature ($T = 300$ K) are presented in Fig. 3(c). We clearly observed two exponential decays, with fast PL decay (transient lifetime $\tau_f = 83$ ns) and slow decay ($\tau_d = 2.7$ μs) components. We note that the latter τ_d is comparable to that of conventional Ir complexes such as iridium 2-phenylpyridine [$Ir(ppy)_3$] derivatives with $\tau = 1$–5 μs [12], indicating that PIC-TRZ2 has comparable transient performance of delayed fluorescence to those of Ir complexes. In a separate experiment, to confirm the nearly zero gap formation, we measured the temperature dependence of the radiative decay rate of the delayed fluorescence ($k_{r(\mathrm{TADF})}$) [see Fig. 4(d)], determining an activation energy of $\Delta E_{\mathrm{ST}} = 0.02$ eV.

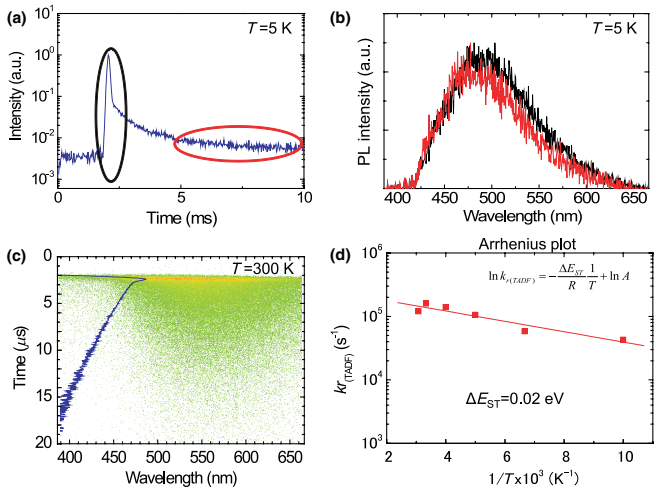

FIG. 3 (color online). (a) Photoluminescence decay characteristics of 6 wt % PIC-TRZ2: mCP, and (b) emission spectra of prompt (black line) and delayed (red line) components at $T = 5$ K. Spectra corresponded well with each other, indicating that the delayed component is caused by TADF. (c) Photoluminescence decay characteristics of 6 wt % PIC-TRZ2: mCP at room temperature ($T = 300$ K), indicating the presence of clear two exponential decays with transient lifetimes of 83 ns and 2.7 μs. (d) Temperature dependence of the radiative decay rate of the TADF component, indicating $\Delta E_{\mathrm{ST}} = 0.02$ eV.

To maximize the TADF efficiency of films doped with PIC-TRZ2, we optimized the host materials. Figure 4 and Table I summarize the PL quantum efficiencies of the total (black), prompt (red), and delayed (green) components of 6 wt %-PIC-TRZ2 doped into host materials with different triplet energies ranging from 2.33 to 3.50 eV. In the case of an N,N'-bis[4′-(diphenylamino)[1,1′-biphenyl]-4-yl]-N,N'-diphenyl-[1,1′-biphenyl]-4,4′-diamine (TPT1) host layer with $T_1 = 2.33$ eV, which is lower than that of PIC-TRZ2, we obtained a low Φ_{PL} of $21 \pm 3\%$ with virtually no appearance of the delayed component. Using 1,1-bis [4-[N,N'-di(p-tolyl)amino]phenyl]cyclohexane (TAPC) ($T_1 = 2.87$ eV), 9,9′-(2,6-pyridinediyl)bis-9H-Carbazole (PYD2) $T_1 = 2.90$ eV) and mCP ($T_1 = 2.91$ eV) as host layers, we obtained significantly higher values of $\eta_{\mathrm{PL}} = 60 \pm 2\%$, $45 \pm 2\%$ and $41 \pm 2\%$, respectively. Bis(2-[(oxo)diphenylphosphino]phenyl)ether (DPEPO) and 1,4-bis(triphenylsilyl)benzene (UGH2) host layers with higher T_1 of >3.0 eV clearly showed the appearance of the delayed components with rather high $\Phi_{\mathrm{PL}} = 51 \pm 2\%$ and $59 \pm 2\%$, respectively. Transient PL measurements revealed that the use of a host with higher triplet energy

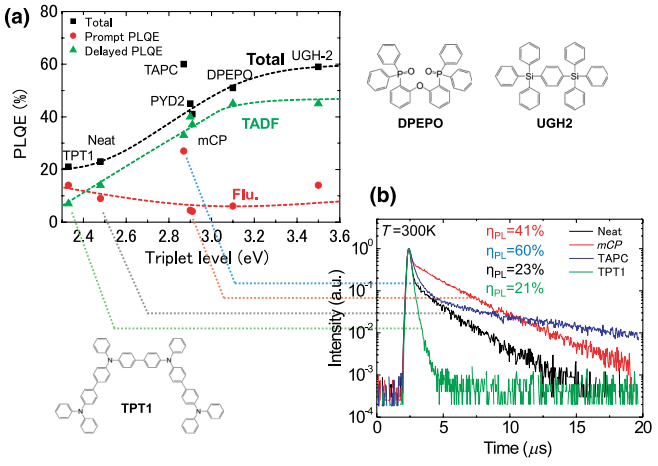

FIG. 4 (color online). (a) Photoluminescence quantum efficiency (PLQE) of PIC-TRZ2 at $T = 300$ K in various host layers with different triplet energies. Total PLQE (black) is the sum of QE based on prompt fluorescence efficiency (red) and QE based on TADF (green). (b) Corresponding transient decay curves in mCP (red), TPT1 (green), and TAPC (blue) host layers and a neat film (black).

than that of the dopant allowed the delayed components to be observed, indicating improved confinement of the triplet excitons of PIC-TRZ2 leads to intense delayed fluorescence. Conversely, hosts with a triplet energy lower than that of PIC-TRZ2 allow partial triplet energy transfer from the guest to the host molecules, which is lost as nonradiative decay. In the case of PIC-TRZ2:UGH2, a total PL efficiency of 59% ± 2% with 45% ± 2% from the delayed component and 14% ± 2% from the prompt component was obtained. Because the PL efficiency of the prompt component exhibited almost no temperature dependence, it is possible that nonradiative decay from the S_1 excited state is negligible and ca. 40% is nonradiatively deactivated from the T_1 excited state. We noted that exceptional behavior was observed using TAPC as a host. Despite the low triplet energy of TAPC, the doped film exhibited rather high PL efficiency. We suppose that the rather long lifetime of triplet excitons in TAPC would promote back energy transfer from host to guest molecules after energy transfer from guest to host molecules and successive energy migration between TAPC molecules [24]. This unanticipated behavior will be clarified in a separate experiment.

Next, we fabricated OLEDs containing PIC-TRZ2 and improved their EL characteristics by optimizing carrier transport and host layers. (See the Supplemental Material [25] for detailed device structures and additional information on OLED performance of current-density (J)–voltage and EL spectra). As the first trial, we deposited α-NPD (40 nm) as a hole transport layer, mCP (10 nm) as an exciton blocking layer, 6 wt % PIC-TRZ2: mCP or PIC-TRZ2:DPEPO (20 nm) as an emitter layer, 4,7-diphenyl-1,10-phenanthroline (Bphen) or DPEPO (40 nm) as an electron transport layer and finally LiF (1 nm) and Al (80 nm) layers as a cathode on an indium tin oxide (ITO, 100 nm) substrate layer (devices I–IV). The devices exhibited blue-green emission with a maximum at around 505 nm and the maximum EL efficiency of $\eta_{EQE} = 8.0\% \pm 1\%$ was obtained in device II [Fig. 5(a)]. This value clearly exceeds the theoretical limitation of $\eta_{EQE} = 2.0\%$ assuming only conventional fluorescence with a PL quantum efficiency of $\Phi_{PL} = 40\%$ from PIC-TRZ2.

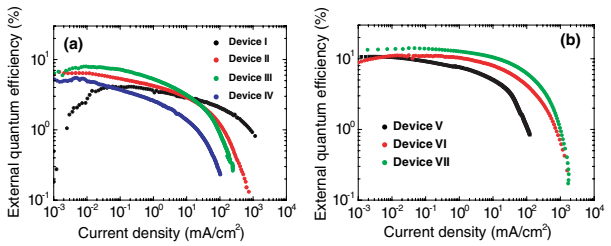

FIG. 5 (color online). OLED characteristics of five devices using PIC-TRZ2 as an emitter under steady-state conditions. η_{ext}-J characteristics for devices (a) I–IV, and (b) V–VII. The highest external EL efficiency of 14.0% ± 1% was achieved for device V.

However, if energy transfer occurs readily, we can expect a further enhancement of η_{EQE}, suggesting a theoretical maximum of 11.8%. We attributed the obtained lower value to unbalanced carrier injection and transport in addition to exciton migration into adjacent carrier transport layers, i.e., imperfect triplet exciton confinement. Thus, we tried to optimize the device parameters to maximize η_{EQE}.

Further, we also examined TAPC as a host layer because the doped film exhibited a rather high Φ_{PL} of 60% ± 3%, but it did not enhance η_{EQE}, probably because of undesirable electroplex formation [26]. While TAPC is unsuitable as a host in the emitter layer in this case, we found that it caused a pronounced decrease of driving voltage. Thus, we used TAPC as a hole transport layer instead of a host layer.

Next, we prepared devices V, VI, and VII by incorporating DPEPO as an electron transport layer and TAPC as a hole transport layer. We used PYD2 as a host layer to enhance electron transport ability of the emitter layer. We further optimized the electron transport layer by using 2,2′,2″-(1,3,5-phenylene)tris(1-phenyl-1*H*-benzimidazole) and 1,3,5-tris(3-pyridyl-3-phenyl)benzene, so the structures of the devices were as follows: device V: ITO/TAPC (40 nm)/PYD2 : 6 wt % PIC-TRZ2 (20 nm)/DPEPO (5 nm)/DPEPO (45 nm)/LiF/Al, Device VI: ITO/TAPC (40 nm)/PYD2 : 6 wt % PIC-TRZ2 (20 nm)/DPEPO (5 nm)/TPBi (45 nm)/LiF/Al, and device VII: ITO/TAPC (40 nm)/PYD2 : 6 wt % PIC-TRZ2 (20 nm)/DPEPO (5 nm)/TmPyPBi (45 nm)/LiF/Al.

Figure 5(b) shows η_{ext}-J characteristics for the devices. Using TmPyPBi as an electron transport layer, we obtained $\eta_{ext} = 14.0\% \pm 1\%$ at $J = 0.04$ mA/cm^2 and $\eta_{ext} = 11\% \pm 1\%$ at $J = 1$ mA/cm^2, which is the highest value ever reported for PIC-TRZ based TADF devices. Because the PL quantum efficiency of 6 wt % PIC-TRZ2: PYD2 is

TABLE I. PL characteristics of PIC-TRZ2 in host layers with different triplet energies.

	PLQE (%)	Prompt PLQE (%)	Delayed PLQE (%)	Triplet level (eV)	Emission peak (nm)
Neat	23	9.0	14	2.48	500
TPT1[a]	21	14	7.0	2.33	517
TAPC[b]	60	27	33	2.87	533
PYD2[c]	45	4.5	40	2.90	506
mCP[d]	41	4.1	37	2.91	504
DPEPO[e]	51	6.1	45	3.10	490
UGH2[f]	59	14	45	3.50	487

[a]*N*,*N*′-bis[4′-(diphenylamino)[1,1′-biphenyl]-4-yl]-*N*,*N*′-diphenyl-1-[1,1′biphenyl].
[b]1,1-bis(4-(*N*,*N*-di(p-tolyl)amino)phenyl)-cyclohexane.
[c]3,5-Di(9*H*-carbazol-9-yl)-pyridine.
[d]*N*,*N*′-4,4′-dicarbazole-3,5-benzene.
[e]Bis(2-(diphenylphosphino) phenyl)ether oxide.
[f]1,4-Bis(tri-phenylsilyl)benzene.

45% ± 3%, this result suggests that the exciton formation efficiency reached its ultimate value of 100% based on the exciton formation formula under electrical excitation [15], even assuming a light out-coupling efficiency of $\eta_{out} \sim 30\%$, which is the upper limit [27] (See caption of Fig. 1). We note that such high η_{out} would be ascribed to the horizontal molecular orientation against a substrate [28]. Thus, we succeeded in harvesting all electrically generated excitons as radiative decay.

Here we discuss the position of PIC-TRZ2 as an organic luminescent material. PIC-TRZ2 possesses ΔE_{ST} of almost zero. In fact, the formation of small energy gap is widely known in phosphorescence materials such as ketones, e.g., benzophenone and their derivatives [29]. A general feature of the emission of ketones with n-π^* states is very small fluorescence efficiencies of $\Phi_f < 0.001$. Because the n-π^* transition means that the overlap integral between the ground and excited states is small, the radiative decay rate of singlet excitons is just $k_r \sim 10^5\ s^{-1}$, which is much smaller than those of competing deactivation processes such as the intersystem crossing rate of $k_{ST} \sim 10^{11}\ s^{-1}$, resulting in almost no fluorescence. Thus, it is generally accepted that both high Φ_f and small ΔE_{ST} is infeasible in organic molecules. However, while PIC-TRZ2 has nearly zero-gap energy, a rather high Φ_f of ~60% was obtained. This is because PIC-TRZ2 has appreciable oscillator strength (density functional theory calculation estimated an oscillator strength of $f = 0.0012$) and the apparent radiative decay rate of TADF in 6 wt % PIC-TRZ: mCP is $k_{TADF} \sim 10^6\ s^{-1}$, which is comparable with those of $Ir(ppy)_3$ derivatives showing room temperature phosphorescence of nearly 100% [30]. While $k_{TADF} \sim 10^6\ s^{-1}$ is not high compared with $\sim 10^{8-9}\ s^{-1}$ of conventional fluorescent molecules, once the emitters are dispersed in a rigid solid-state matrix, we can obtain pragmatic TADF efficiency. Thus, PIC-TRZ2 breaks the current view of luminescent materials, suggesting that appropriate arrangement of donor and acceptor moieties in molecular structures can allow both zero gap and feasible oscillator strength, leading to highly efficient TADF.

This work was supported by a Grant-in-aid from the Funding Program for World-Leading Innovative R&D on Science and Technology (FIRST) and the International Institute for Carbon Neutral Energy Research (WPI-I2CNER) sponsored by the Ministry of Education, Culture, Sports, Science and Technology.

[1] N. C. Shaner, G. H. Patterson, and M. W. Davidson, J. Cell Sci. **120**, 4247 (2007).
[2] H. Klauk, *Organic Electronics* (Wiley-VCH Verlag GmbH & Co. KGaA, New York, 2006).
[3] K. Müllen, and U. Scherf, *Organic Light-Emitting Devices* (Wiley-VCH Verlag GmbH & Co. KGaA, New York, 2006).
[4] W. Brütting, *Physics of Organic Semiconductors* (Wiley-VCH Verlag GmbH & Co. KGaA, New York, 2005).
[5] H. Yersin, *Highly Efficient OLEDs with Phosphorescent Materials* (Wiley-VCH Verlag GmbH & Co. KGaA, New York, 2008).
[6] S. Chen, L. Deng, J. Xie, L. Peng, L. Xie, Q. Fan, and W. Huang, Adv. Mater. **22**, 5227 (2010).
[7] D. K. Flattery, C. R. Fincher, C. R. LeCloux, M. B. O'Regan, and J. C. Richard, Information Display **10–11**, 8 (2011).
[8] P. A. Levermore, V. Adamovich, K. Rajan, W. Yeager, C. Lin, S. Xia, G. S. Kottas, M. S. Weaver, R. Kwong, R. Ma, M. Hack, and J. J. Brown, SID Symp. Dig. Tech. Papers **41**, 786 (2010).
[9] J. W. Park, D. C. Shin, and S. H. Park, Semicond. Sci. Technol. **26**, 034002 (2011).
[10] M. A. Baldo, S. Lamansky, P. E. Burrows, M. E. Thompson, and S. R. Forrest, Appl. Phys. Lett. **75**, 4 (1999).
[11] C. Adachi, M. A. Baldo, M. E. Thompson, and S. R. Forrest, J. Appl. Phys. **90**, 5048 (2001).
[12] S. Lamansky, P. Djurovich, D. Murphy, F. Abdel-Razzaq, H-E. Lee, C. Adachi, P. E. Burrows, S. R. Forrest, and M. E. Thompson, J. Am. Chem. Soc. **123**, 4304 (2001).
[13] P. Laznicka, *Giant Metallic Deposits* (Springer-Verlag, Berlin, Heidelberg, 2006).
[14] J. Lee, C. H. Park, J. Kwon, S. C. Yoon, L.-M. Do, and C. Lee, Synth. Met. **162**, 1961 (2012).
[15] A. Endo, M. Ogasawara, A. Takahashi, D. Yokoyama, Y. Kato, and C. Adachi, Adv. Mater. **21**, 4802 (2009).
[16] A. Endo, K. Sato, K. Yoshimura, T. Kai, A. Kawada, H. Miyazaki, and C. Adachi, Appl. Phys. Lett. **98**, 083302 (2011).
[17] S. Lee, T. Yasuda, H. Nomura, and C. Adachi, Appl. Phys. Lett. **101**, 093306 (2012).
[18] K. Goushi, K. Yoshida, K. Sato, and C. Adachi, Nat. Photonics **6**, 253 (2012).
[19] T. Nakagawa, S.-Y. Ku, K.-T. Wong, and C. Adachi, Chem. Commun. (Cambridge) **48**, 9580 (2012).
[20] M. Gabor, H. Nomura, Q. Zhang, T. Nakagawa, and C. Adachi, Angew. Chem. **51**, 11 311 (2012).
[21] H. Tanaka, K. Shizu, H. Miyazaki, and C. Adachi, Chem. Commun. (Cambridge) **48**, 11 392 (2012).
[22] Q. Zhang, J. Li, K. Shizu, S. Huang, S. Hirata, H. Miyazaki, and C. Adachi, J. Am. Chem. Soc. **134**, 14 706 (2012).
[23] H. Uoyama, K. Goushi, K. Shizu, H. Nomura, and C. Adachi, Nature (London) **492**, 234 (2012).
[24] Y. Kawamura, K. Goushi, J. Brooks, J. J. Brown, H. Sasabe, and C. Adachi, Appl. Phys. Lett. **86**, 071104 (2005).
[25] See Supplemental Material at http://link.aps.org/supplemental/10.1103/PhysRevLett.110.247401 for details on OLED characteristics and DFT calculation.
[26] H. Zhu, Z. Xu, F. Zhang, S. Zhao, and D. Song, Appl. Surf. Sci. **254**, 5511 (2008).
[27] M. Furno, R. Meerheim, S. Hofmann, B. Lüssem, and K. Leo, Phys. Rev. B **85**, 115205 (2012).
[28] J. Frischeisen, D. Yokoyama, C. Adachi, and W. Brütting, Appl. Phys. Lett. **96**, 073302 (2010).
[29] N. J. Turro, *Modern Molecular Photochemistry* (University Science Books, Sausalito, 1991).
[30] A. Endo and C. Adachi, Chem. Phys. Lett. **483**, 224 (2009).